Cognitive Waveform and Receiver Selection Mechanism for Multistatic Radar

Moez Ben Kilani, Yogesh Nijsure, Ghyslain Gagnon, Georges Kaddoum and François Gagnon

LACIME Laboratory, École de technologie supérieure, 1100 Notre-Dame West, H3C 1K3, Montreal, Canada

*moez.b.kilani@gmail.com

Abstract

A novel Cognitive Radar (CR) approach to improve the extended targets detection and resolution is developed in a multistatic radar context. A cognitive waveform selection mechanism based on target probability of detection maximization in conjunction with adaptive receiver allocation/selection is proposed. Apart from the cognitive waveform selection objective, this process aims at evaluating the optimal positions for the radar receivers in an attempt to iteratively minimize the Geometric Dilution of Precision (GDOP), subsequently resulting in a high precision target geolocation estimate. The cognitive waveform selection mechanism is based on target dynamics involving time varying target scattering characteristics and clutter distribution parameters. Thus with the proposed dual objective approach, the concept of cognition can be extended to both the radar transmitter and receiver sites. Numerical results demonstrate better target detection performance and positioning accuracy using the proposed approach as compared with conventional methods based on static transmission or stationary multistatic receivers topology.

Keywords: Cognitive radar, multistatic, waveform selection, GDOP, extended target.

I. INTRODUCTION

Cognitive Radar (CR) is an innovative paradigm for optimizing traditional radar performances within dynamic environments [1]. The concept is essentially based on a continuous learning through radar interactions with its surrounding world, and an iterative feedback from the receiver to the transmitter facilitates the adaptation of radar transmission parameters in real time [1]. The continuous target tracking is ensured by preservation of the information content of the radar returns [1]. The reaction of the transmitter to the updated information coming from the feedback loop has a crucial impact on the ability of the CR to intelligently adapt to the environment. As a result, a lot of the research efforts have been focused on the waveform design and optimization. Waveform optimization was emphasized by the need to properly detect extended targets. In contrast to point targets, which have a flat response across the operating frequency band of the radar, extended targets exhibit random scattering characteristics due to their range extent. Thus, optimal waveform could be designed in order to maximize the energy reflected from the target.

The topic of CR waveform optimization has been treated following several optimization criteria. A principal waveform design approach is to directly optimize the receiver detection statistics of extended targets in the presence of clutter and additive noise. In [2]–[4], the dynamic choice of both the waveform and the receiver impulse response is dictated by a maximization process

of the output Signal-to-Clutter plus Noise Ratio (SCNR). in [5], the Neyman-Pearson (NP) detector is derived in case of extended target and clutter. The detailed waveform design process is based on a maximization process of the symmetrized Kullback-Liebler measure directly linked to the target detection performance. A Generalized Canonical Correlation (GCC) detector for multistatic passive detection is proposed in [6]. It is shown that the proposed detector performs better than the Generalized Likelihood Ratio Test (GLRT) detector only in case of known noise statistics [6]. A comparative study between the Adaptive Matched Filter (AMF) detector and the GLRT detector is carried out in [7], It is shown that the GLRT outperforms AMF in case of unknown noise and target scattering statistics. Both detectors exibit better performances with an increasing number of receiver platforms [7].

Multistatic radars offer many advantages compared to monostatic radars especially increased coverage and improved target resolution and classification [8], in addition to higher tolerance to sources of interference due to their spatial diversity and the potential for improved physical survivability owing to the multiplicity of stations [9]. However, a minimum level of synchronization between different units is required to achieve multistatic signal processing [9].

Geometric Dilution of Precision (GDOP) is a metric initially used in satellite navigation to characterize the impact of system geometry on the positioning accuracy [10]. Recently applied to general sensor network systems design [11]–[13], GDOP is defined as the ratio of the root-mean-square position error to the root-mean-square ranging error [12]. Consequently, higher GDOP value for a particular topological distribution of the sensor networks represents poor positioning performance. From the above GDOP definition, a good positioning accuracy could be achieved with an optimal choice of the sensor network geometry.

Following from the above discussions, it is interesting to study the performances of cognitive multistatic radar where the selection of the transmitted waveform and the placement of the receivers are dynamically changed to adapt to the time-varying environment. Some works [14]–[16] relate to the optimization of the multistatic radar geometry for enhanced target positioning accuracy. In [14], the selection of two transmitters of opportunity and a single receiver location in a passive multistatic radar is performed using a Cramer-Rao Lower Bound (CRLB) based algorithm, which considers a set of constraints for the relative positions of the transmitter and receiver units. The proposed solution is considered accurate but computationally expensive [14]. A joint approach based on transmitter waveform and receiver path optimization for target tracking by multistatic radar is proposed in [16]. The developed algorithm minimizes the tracking mean square error, however it doesn't account for extended target processing. In addition, the environment is assumed to be clutter free. In our work context, we propose a joint approach to optimize both detection and positioning accuracy of extended targets in clutter plus noise corrupted environment.

The contributions of the current work can be summarized as:

1) Design of a cognitive waveform selection mechanism, based on the principle of maximization of target detection probability.

2) Development of a receiver positioning strategy, with an objective of GDOP minimization, which supplements the previous contribution concerning cognitive waveform selection.

3) Fusion of both parts to form a hybrid system that shows better detection performances in comparison with only the cognitive waveform selection mechanism.

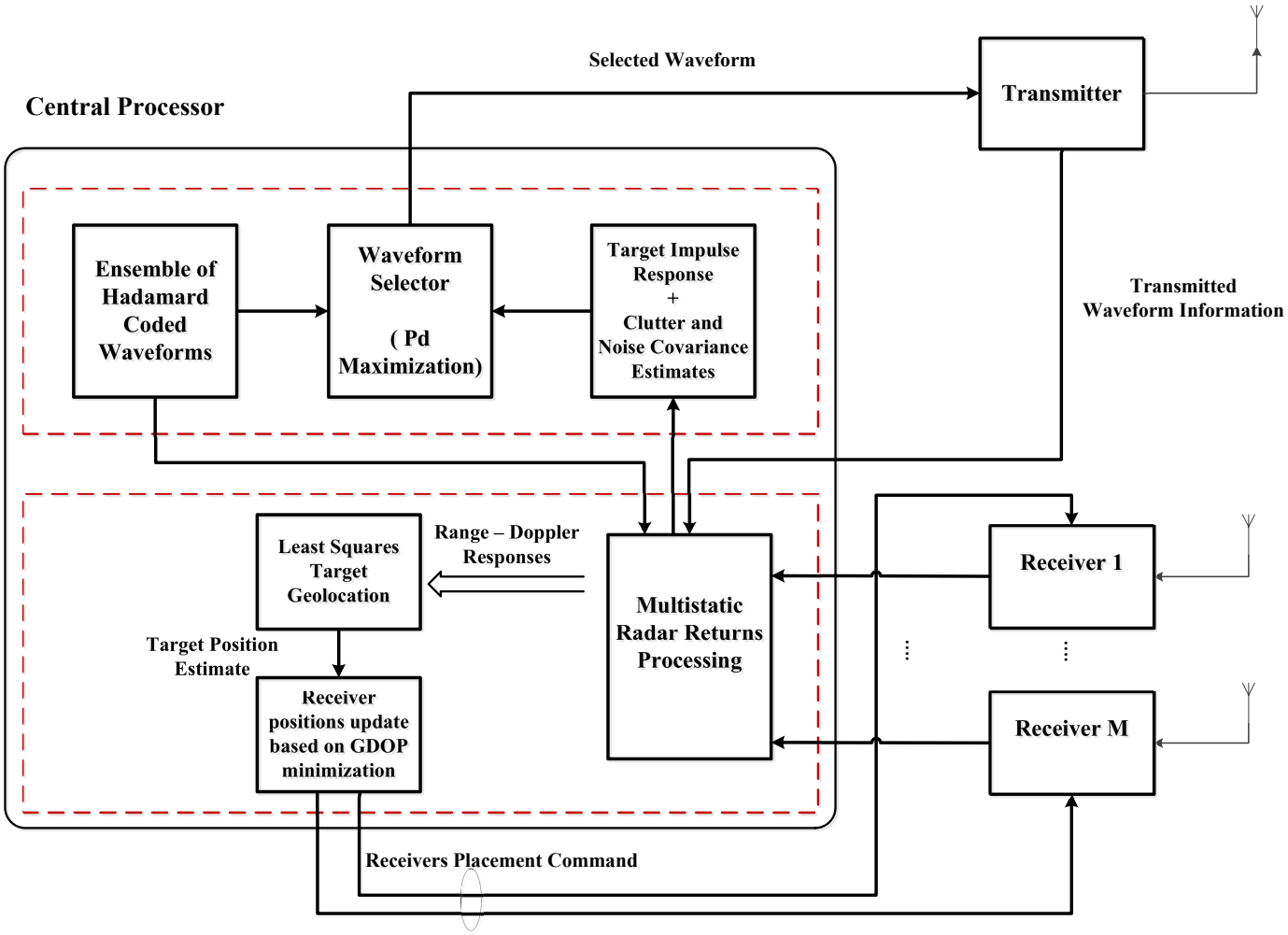

Fig. 1. Proposed CR architecture.

The remainder of the paper is organized as follows, In Section II, we describe the system architecture. In Section III, we present the signal model and the waveform selection process. We describe in Section IV, the Least Squares (LS) geolocation process used to estimate the target absolute position and velocity and we detail the GDOP based receiver locations update strategy. Section V shows the numerical results for different parts of the proposed cognitive framework. Finally, some concluding remarks are drawn in Section VI.

II. System Architecture

Fig. 1 shows the general architecture of the proposed CR system. The cognitive loop could be summarized in the following steps:

Step I The backscattered signals gathered from different receivers are matched filtered in the multistatic radar returns processing block where the received signals are correlated with the transmitted waveform. Consequently, the outputs of the matched filtering process are used to estimate the target impulse responses in addition to the clutter and noise covariances through successive measurements. Then, the central processor uses the estimated dynamic radar scene information to select the waveform that maximizes the probability of target detection. The waveform selector block in the central processor chooses

the waveform to transmit within an ensemble of Hadamard phase coded waveforms according to the detection maximization criterion.

$Step\ II$ The range-Doppler responses relative to different bistatic transmitter-receiver pairs are computed after matched filtering. Subsequently, multiple information relative to bistatic target ranges and bistatic Doppler shifts are extracted from different range-Doppler responses and injected into a LS geolocation process in order to compute the absolute position and velocity estimates of the target. The target position estimate is then used to compute the GDOP of the target positioning algorithm. Finally, a GDOP-based minimization approach is carried out in order to obtain the optimal positions of the receivers according to the actual target position estimate.

$Step\ III$ The central processor sends a waveform selection command to the transmitter in order to transmit the waveform chosen according to $Step\ I$. Meanwhile, the central processor will evaluate the optimal positions obtained from $Step\ II$ and will instruct the receivers to update their locations accordingly in real-time as shown in Fig. 1.

Different steps are then repeated iteratively allowing the cognitive system to continuously adapt its operational mode to the dynamic scene.

III. Signal Model

In this work, we use phase-coded waveforms as they can fully exploit the transmit power with sufficient variability unlike traditional Linear Frequency Modulated (LFM) waveforms [17]. Each phase-coded waveform comprises a train of phase-coded Gaussian pulses. Each pulse is divided into $N = 512$ subpulses each of duration $\delta = 6.6$ ns. A unimodular Hadamard code is used to modulate the phases of the subpulses, which corresponds to a specific row of the $N \times N$ Walsh-Hadamard matrix. Hadamard sequences with sufficient length are chosen in order to improve the Doppler resolution of the radar system. Each normalized Gaussian pulse takes the following form:

$$f(t) = \frac{1}{\sqrt{2\pi}T} \exp\left(\frac{-t^2}{T^2}\right), \tag{1}$$

where T is the pulse width.

We denote by $f_n(t)$ the n^{th} subpulse of the pulse $f(t)$. The complex envelope of one transmitted phase-code pulse is expressed as:

$$I(t) = \sum_{n=1}^{N} c_n f_n(t), \tag{2}$$

where c_n is the Hadamard sequence code of the subpulse $f_n(t)$. The transmitted burst is a train of U phase-coded pulses (i.e., delayed versions of $I(t)$) given by:

$$s(t) = \sum_{u=1}^{U} I(t - uT_{PR}), \tag{3}$$

where $s(t)$ is the complex envelope of the narrowband transmitted signal and T_{PR} is the pulse repetition time.

We consider M physically separated receive sensors so that all the received clutter and noises are statistically independent from one sensor to sensor.

We denote by $x_i(t)$ the complex input of the i^{th} receiver, $c_i(t)$ denotes clutter and $n_i(t)$ the sum of ambient noise and interference, i.e., jamming. $n_i(t)$ and $c_i(t)$ are modelled as zero mean complex wide sense stationary (WSS) Gaussian random processes.

The detection problem of an extended target in the presence of clutter and noise can be summarized as:

$$\begin{aligned} H_0 &: x_i(t) = c_i(t) + n_i(t) \\ H_1 &: x_i(t) = [h_i(t) * s(t)] + c_i(t) + n_i(t), \end{aligned} \tag{4}$$

where H_0 is the hypothesis of target absence (i.e., only clutter and noise are present), H_1 is the hypothesis of target presence in addition to clutter and noise, $h_i(t)$ is the extended target impulse response relative to the i^{th} receiver and $*$ denotes convolution. For ease of illustration, we suppose that the clutter is stationary.

We consider the Swerling I target model, which implies that the target is made up of many independent scatterers of roughly equal areas. Under such assumption, the backscattered signal coming from the target can be expressed as:

$$\begin{aligned} h_i(t) * s(t) &= A_i[g_i(t) * s(t)] \\ &= A_i \sum_{k=1}^{N_s} b_{ik} s(t - \tau_{ik}) \exp(2\pi j f_{ik} t), \end{aligned} \tag{5}$$

where A_i is a complex reflection factor proportional to the extended target Radar Cross Section (RCS) with the Probability Density Function (PDF) $A_i \sim CN(0, \sigma^2_{A_i})$, $g_i(t)$ is the deterministic part of the extended target impulse response, N_s represents the number of scatterers composing the target, b_{ik} is a deterministic coefficient relative to the k^{th} scatterer and the i^{th} path, τ_{ik} is the total delay experienced by the transmitted signal from the transmitter to the i^{th} receiver and after reflection by the k^{th} scatterer in between and f_{ik} represents the bistatic Doppler shift experienced by the transmitted signal along the i^{th} path and caused by the movement of the k^{th} scatterer. Consequently the expression of the received signal at the i^{th} receiver under Hypothesis H_1 is now derived as:

$$x_i(t) = A_i \sum_{k=1}^{N_s} b_{ik} s(t - \tau_{ik}) \exp(2\pi j f_{ik} t) + c_i(t) + n_i(t). \tag{6}$$

We take Q samples of each received signal $x_i(t)$ and we define the vector $\mathbf{X_i}, i = 1, ..., M$ of dimension $1 \times Q$, which is composed of the received samples. Also, we define the column vector of all sensor outputs $\mathbf{X} = [\mathbf{X_1}, ..., \mathbf{X_M}]^T$. Hence the detection problem of (4) can be represented as:

$$\begin{aligned} H_0 &: \mathbf{X_i} = \mathbf{C_i} + \mathbf{N_i} \\ H_1 &: \mathbf{X_i} = \mathbf{T_i} + \mathbf{C_i} + \mathbf{N_i} \\ &= A_i \mathbf{G_i} + \mathbf{C_i} + \mathbf{N_i}, \end{aligned} \tag{7}$$

where $c_i(t)$ and $n_i(t)$ are replaced by their corresponding column vectors of samples $\mathbf{C_i}$ and $\mathbf{N_i}$, $\mathbf{T_i}$ denotes the vector of backscattered signal samples coming from the target and $\mathbf{G_i}$ is the vector of samples related to the deterministic part of the

target response $g_i(t) * s(t)$. It follows that $\mathbf{T_i}$,$\mathbf{C_i}$ and $\mathbf{N_i}$ are all complex multivariate Gaussian random vectors with a zero mean vector. The PDF of the received vector $\mathbf{X_i}$ under H_0 is given by [5]:

$$p(\mathbf{X_i}; H_0) = \frac{1}{\pi^Q det(\mathbf{K_i})} \exp[-\mathbf{X_i}^H \mathbf{K_i}^{-1} \mathbf{X_i}], \tag{8}$$

where $\mathbf{K_i}$ is the covariance matrix of $\mathbf{C_i} + \mathbf{N_i}$. Since A_i ,$\mathbf{C_i}$ and $\mathbf{N_i}$ are assumed independent of each other, the PDF under H_1 can be represented as [5]:

$$\begin{aligned} p(\mathbf{X_i}; H_1) = & \frac{1}{\pi^Q det(\sigma_{A_i}^2 \mathbf{G_i} \mathbf{G_i}^H + \mathbf{K_i})} \\ & \times \exp[-\mathbf{X_i}^H (\sigma_{A_i}^2 \mathbf{G_i} \mathbf{G_i}^H + \mathbf{K_i})^{-1} \mathbf{X_i}]. \end{aligned} \tag{9}$$

Furthermore all sensor outputs $\mathbf{X_i}$ are considered independent. Thus,

$$p(\mathbf{X}; H_w) = \prod_{i=1}^{M} p(\mathbf{X_i}; H_w), \quad w = 0, 1 \tag{10}$$

After deriving the distribution of the NP detection statistic, the probability of false alarm P_{FA} and detection P_D expressions can be obtained following the derivations in [5]:

$$P_{FA} = \sum_{i=1}^{M} P_i \exp[-\gamma/(2\alpha_i^{(0)})] \tag{11}$$

$$P_D = \sum_{i=1}^{M} Q_i \exp[-\gamma/(2\alpha_i^{(1)})], \tag{12}$$

where

$$P_i = \prod_{n=1 \ n \neq i}^{M} \frac{1}{1 - \alpha_n^{(0)}/\alpha_i^{(0)}} \tag{13}$$

$$Q_i = \prod_{n=1 \ n \neq i}^{M} \frac{1}{1 - \alpha_n^{(1)}/\alpha_i^{(1)}} \tag{14}$$

and

$$\alpha_i^{(0)} = \frac{\sigma_{A_i}^2 \mathbf{G_i}^H \mathbf{K_i}^{-1} \mathbf{G_i}}{1 + \sigma_{A_i}^2 \mathbf{G_i}^H \mathbf{K_i}^{-1} \mathbf{G_i}} \tag{15}$$

$$\alpha_i^{(1)} = \sigma_{A_i}^2 \mathbf{G_i}^H \mathbf{K_i}^{-1} \mathbf{G_i} \tag{16}$$

The weighting term $\alpha_i^{(0)}$ characterizes the contribution of the i^{th} receiver in the detection process. If a small target return is measured at the i^{th} receiver (i.e., $\sigma_{A_i}^2 \mathbf{G_i}^H \mathbf{K_i}^{-1} \mathbf{G_i} \ll 1$), then its contribution will not be included in the detection decision.

As a result, the proposed approach allows to efficiently leverage the signal diversity offered by the multistatic topology in order to optimize the target detection capabilities.

Following from the above discussions, a multistatic cognitive waveform selection process could be devised in order to maximize the probability of detection expressed in (12) for a given probability of false alarm. Indeed, the threshold value γ could be dynamically derived by solving (11) for a fixed value of the probability of false alarm and the real-time scene parameters (i.e., the extended target impulse responses in addition to clutter plus noise covariance estimates). The resulting threshold γ is then used to compute the probability of detection.

The waveform selection process could be formulated as:

$$s_{opt} = \max_{s_k \in S} P_D, \tag{17}$$

where s_{opt} is the selected waveform that maximizes P_D, S is the ensemble of Hadamard phase-coded sequences and s_k is a particular probing waveform from S.

The probability of target detection is maximized at each iteration. Subsequently, new waveform is selected for transmission. Each waveform is composed of a train of Hadamard phase-coded pulses where the subpulses coding sequence corresponds to a specific Hadamard sequence as described in section III. The procedure of cognitive waveform selection could be summarized as follows:

1) Select a waveform from the ensemble S for transmission.

2) The received signals are used to estimate the real-time covariance matrices of clutter and noise $\mathbf{K_i}$ in addition to the extended target impulse responses and scattering coefficient variances $\sigma^2_{A_i}$ corresponding to the i^{th} receiver.

3) For each waveform s_k in the ensemble S, use the information regarding actual Doppler shifts and total delays contained in the estimated target impulse responses to compute the deterministic vectors $\mathbf{G_i}$ relative to s_k as detailed in (6) and (7). Then compute the actual values of $\alpha_i^{(0)}$ and $\alpha_i^{(1)}$ in (15) and (16) based on the current estimates of $\mathbf{G_i}$, $\mathbf{K_i}$ and $\sigma^2_{A_i}$ and update the threshold γ by solving (11) for the fixed value of probability of false alarm P_{FA}. Finally calculate the value of P_D, which corresponds to the waveform s_k based on actual values of $\alpha_i^{(0)}$, $\alpha_i^{(1)}$ and γ as described in (12).

4) Choose the waveform s_{opt} corresponding to the maximum P_D.

5) Transmit s_{opt}, collect the return signals and process it in each receiver. Repeat steps 2-5.

IV. Multistatic GDOP Based receiver locations update Strategy

A. Least Squares Geolocation Process

The backscatter signals coming from the target are matched filtered at each receiver and the bistatic range-Doppler responses relative to different receivers are processed. Consequently bistatic ranges and Doppler shifts relative to different transmitter-receiver pairs could be easily extracted from the range-Doppler responses. Theoretical expressions of bistatic range and bistatic Doppler shift are given by [17]:

$$r_i = \sqrt{R_T \times R_{ri}}, \tag{18}$$

$$\begin{aligned} f_i &= 2\frac{V}{\lambda}\cos\phi_i\cos(\beta_i/2) \\ &= 2\frac{V}{\lambda}\cos\phi_i\sqrt{1/2+\frac{R_T - L_i\sin\theta_T}{2\sqrt{R_T^2+L_i^2-2R_TL_i\sin\theta_T}}}, \end{aligned} \tag{19}$$

Where r_i is the bistatic range relative to the transmitter and the i^{th} receiver, R_T is the transmitter to target range, R_{ri} is the i^{th} receiver to target range. f_i is the bistatic Doppler shift, L_i is the baseline separating the transmitter from the i^{th} receiver, $V = \sqrt{v_x^2+v_y^2+v_z^2}$ is the target velocity, λ is the carrier wavelength, β_i is the the bistatic angle, ϕ_i is the angle between the target velocity vector and the bistatic bisector and θ_T is the angle between the transmitter and the target. The aim of the geolocation step is to estimate the absolute target position and velocity from the measured bistatic ranges and Doppler shifts relative to different receivers. The LS geolocation system can be modelled as:

$$\mathbf{Z} = \mathbf{\Psi}(\boldsymbol{\rho}) + \boldsymbol{\eta}, \tag{20}$$

where $\mathbf{Z} = [r_1,\ \ldots\ , r_M\ , f_1\ \ldots\ , f_M]^T$ is the measurement vector, $\boldsymbol{\rho} = [x,\ y,\ z,\ v_x,\ v_y\ , v_z]^T$ is the vector of unknown target parameters (i.e., target position and velocity vectors) and $\boldsymbol{\eta}$ is the measurement noise vector.

From (18), (19) and (20), we can represent the hybrid system as,

$$\mathbf{\Psi} = \begin{bmatrix} \sqrt{R_T \times R_{r1}} \\ \sqrt{R_T \times R_{r2}} \\ . \\ . \\ . \\ \sqrt{R_T \times R_{rM}} \\ 2\frac{\sqrt{v_x^2+v_y^2+v_z^2}}{\lambda}\cos\phi_1\sqrt{1/2+\frac{R_T-L_1\sin\theta_T}{2\sqrt{R_T^2+L_1^2-2R_TL_1\sin\theta_T}}} \\ 2\frac{\sqrt{v_x^2+v_y^2+v_z^2}}{\lambda}\cos\phi_2\sqrt{1/2+\frac{R_T-L_2\sin\theta_T}{2\sqrt{R_T^2+L_2^2-2R_TL_2\sin\theta_T}}} \\ . \\ . \\ . \\ 2\frac{\sqrt{v_x^2+v_y^2+v_z^2}}{\lambda}\cos\phi_M\sqrt{1/2+\frac{R_T-L_M\sin\theta_T}{2\sqrt{R_T^2+L_M^2-2R_TL_M\sin\theta_T}}} \end{bmatrix} \tag{21}$$

The range-velocity estimation problem can be expressed as,

$$\hat{\boldsymbol{\rho}} = \min_{\boldsymbol{\rho}} \parallel \mathbf{Z} - \mathbf{\Psi}(\boldsymbol{\rho}) \parallel . \tag{22}$$

We solve the optimization problem of (22) by using the Trust-Region-Reflective algorithm [18]. The real-time estimate of target position is forwarded to the GDOP based multilateration process in order to optimize the receiver locations for better

target positioning accuracy.

B. GDOP based Receivers Placement Strategy

GDOP is a vital metric, which indicates the efficacy of the sensor network topological distribution in aiding the geolocation process as detailed in works like [11], [19]. Large GDOP values correspond to a poor geometry topology, which will result in poor geolocation performance. Hence, an optimization algorithm is necessary to determine the best set of the sensor locations to be utilized in order to aid the target geolocation process. This optimization would be dynamic and dependent on the current target estimate generated by the LS geolocation process, which has been detailed in the previous section.

The position of the target according to different sensor receivers in the multistatic topology has a crucial impact on the accuracy of target estimation capabilities of the system. Such effects are prominent when the target is very close to or on the bistatic baseline.

In our work context, we assume that the receivers are able to move so that real-time optimal locations could be chosen for better target estimation accuracy. To do so, we devise a multistatic GDOP based optimization approach, which is detailed as follows:

We can express the relationships between the measurement vector and the target parameters as:

$$\mathbf{Z} = \mathbf{F}(\boldsymbol{\zeta}) + \boldsymbol{\eta}, \tag{23}$$

where $\mathbf{Z} = [r_1,\ \dots\ , r_M\ , f_1\ \dots\ , f_M]^T$ is the measurement vector, $\boldsymbol{\zeta} = [x,\ y,\ z]^T$ is the vector of unknown target position coordinates and $\boldsymbol{\eta}$ is the measurement noise vector.

In case of a single extended target and the general case of M receivers, we have,

$$\mathbf{F}(\boldsymbol{\zeta}) = \begin{bmatrix} F_1 \\ F_2 \\ . \\ . \\ . \\ F_M \\ F_{M+1} \\ F_{M+2} \\ . \\ . \\ . \\ F_{2M} \end{bmatrix} = \begin{bmatrix} \sqrt{R_T \times R_{r1}} \\ \sqrt{R_T \times R_{r2}} \\ . \\ . \\ . \\ \sqrt{R_T \times R_{rM}} \\ 2\frac{V}{\lambda}\cos\phi_1 \sqrt{1/2 + \frac{R_T - L_1 \sin\theta_T}{2\sqrt{R_T^2 + L_1^2 - 2R_T L_1 \sin\theta_T}}} \\ 2\frac{V}{\lambda}\cos\phi_2 \sqrt{1/2 + \frac{R_T - L_2 \sin\theta_T}{2\sqrt{R_T^2 + L_2^2 - 2R_T L_2 \sin\theta_T}}} \\ . \\ . \\ . \\ 2\frac{V}{\lambda}\cos\phi_M \sqrt{1/2 + \frac{R_T - L_M \sin\theta_T}{2\sqrt{R_T^2 + L_M^2 - 2R_T L_M \sin\theta_T}}} \end{bmatrix} \tag{24}$$

and the noise vector is expressed as:

$$\boldsymbol{\eta} = \begin{bmatrix} \eta_{r_1} \\ \eta_{r_2} \\ . \\ . \\ . \\ \eta_{r_M} \\ \eta_{f_1} \\ \eta_{f_2} \\ . \\ . \\ . \\ \eta_{f_M} \end{bmatrix} \tag{25}$$

Let the noise covariance matrix be $\boldsymbol{\chi} = E[(\boldsymbol{\eta} - E[\boldsymbol{\eta}])(\boldsymbol{\eta} - E[\boldsymbol{\eta}])^T]$. In order to derive the GDOP for the LS geolocation process $\mathbf{F}$, it is essential to linearize $\mathbf{F}$ by expanding it in a Taylor series about a reference vector $\boldsymbol{\zeta_0} = [x_0,\ y_0,\ z_0]^T$. $\boldsymbol{\zeta_0}$ should be sufficiently close to the actual $\boldsymbol{\zeta}$ (could be an estimate of $\boldsymbol{\zeta}$ determined from a previous iteration).

$$\mathbf{F}(\boldsymbol{\zeta}) = \mathbf{F}(\boldsymbol{\zeta_0}) + \boldsymbol{\Gamma}(\boldsymbol{\zeta} - \boldsymbol{\zeta_0}), \tag{26}$$

where $\boldsymbol{\Gamma}$ is the $2M \times 3$ matrix of derivatives evaluated at $\boldsymbol{\zeta_0}$:

$$\boldsymbol{\Gamma} = \begin{bmatrix} \frac{\partial F_1}{\partial x}\mid_{\zeta_0} & \frac{\partial F_1}{\partial y}\mid_{\zeta_0} & \frac{\partial F_1}{\partial z}\mid_{\zeta_0} \\ \frac{\partial F_2}{\partial x}\mid_{\zeta_0} & \frac{\partial F_2}{\partial y}\mid_{\zeta_0} & \frac{\partial F_2}{\partial z}\mid_{\zeta_0} \\ . & . & . \\ . & . & . \\ . & . & . \\ \frac{\partial F_M}{\partial x}\mid_{\zeta_0} & \frac{\partial F_M}{\partial y}\mid_{\zeta_0} & \frac{\partial F_M}{\partial z}\mid_{\zeta_0} \\ \frac{\partial F_{M+1}}{\partial x}\mid_{\zeta_0} & \frac{\partial F_{M+1}}{\partial y}\mid_{\zeta_0} & \frac{\partial F_{M+1}}{\partial z}\mid_{\zeta_0} \\ \frac{\partial F_{M+2}}{\partial x}\mid_{\zeta_0} & \frac{\partial F_{M+2}}{\partial y}\mid_{\zeta_0} & \frac{\partial F_{M+2}}{\partial z}\mid_{\zeta_0} \\ . & . & . \\ . & . & . \\ . & . & . \\ \frac{\partial F_{2M}}{\partial x}\mid_{\zeta_0} & \frac{\partial F_{2M}}{\partial y}\mid_{\zeta_0} & \frac{\partial F_{2M}}{\partial z}\mid_{\zeta_0} \end{bmatrix} \tag{27}$$

The noise elements composing $\boldsymbol{\eta}$ are assumed independent and identically distributed zero mean Gaussian variables, thus the matrix $\boldsymbol{\chi}$ is diagonal with non zero diagonal elements.

The maximum likelihood or the Least Squares estimator for the linearized model is given by [12]

$$\hat{\boldsymbol{\zeta}} = \boldsymbol{\zeta_0} + (\boldsymbol{\Gamma}^T \boldsymbol{\chi}^{-1} \boldsymbol{\Gamma})^{-1} \boldsymbol{\Gamma}^T \boldsymbol{\chi}^{-1} (\mathbf{Z} - \mathbf{F}(\boldsymbol{\zeta_0})). \tag{28}$$

The covariance matrix of the target parameters estimate vector $\hat{\zeta}$ is computed in [12] as:

$$\mathbf{P} = E[(\hat{\boldsymbol{\zeta}} - E[\hat{\boldsymbol{\zeta}}])(\hat{\boldsymbol{\zeta}} - E[\hat{\boldsymbol{\zeta}}])^T] = (\boldsymbol{\Gamma}^T \boldsymbol{\chi}^{-1} \boldsymbol{\Gamma})^{-1}. \tag{29}$$

Thus from [12], the GDOP can be computed as: $\sqrt{trace[\mathbf{P}]}$.

The choice of the appropriate receiver locations is carried out by minimizing the GDOP at the actual target estimate obtained from the positioning algorithm. Let's denote by Y_i the 3D space where the i^{th} receiver could be located in. Moreover, let the optimum set of receiver locations be represented as $\Lambda = [x_1, y_1, z_1, ..., x_M, y_M, z_M]$. Consequently the minimization problem, which estimates the optimum set of receiver locations Λ for better target positioning accuracy, can be formulated as:

$$\hat{\Lambda} = \min_{(x_i, y_i, z_i) \in Y_i} \; GDOP_{(\hat{x}_a, \hat{y}_a, \hat{z}_a)}, \tag{30}$$

where (x_i, y_i, z_i) are the i^{th} receiver coordinates and $[.]_{(\hat{x}_a, \hat{y}_a, \hat{z}_a)}$ represents the GDOP evaluation at the actual target position estimate, which is obtained from the LS geolocation process. We can solve the non-linear optimization problem of (30) using the interior-point method [20].

V. Simulation Results

In order to validate the proposed approach, a multistatic radar topology of one stationary transmitter and three widely spaced receivers is adopted for all the numerical examples. The transmitter is considered as the reference point and the origin of the system coordinates. We also consider a Swerling I extended target, which consists of seven closely-spaced scatterers moving at the same velocity. The range extent of the target is proportional to the system range resolution, which is the basic condition for extended target consideration as mentioned in [21].

A. Range-Doppler Responses

Fig. 2 shows different range-Doppler plots when an arbitrary waveform from the Hadamard phase-coded waveforms set is selected and transmitted. The bistatic range extents of the slow-moving extended target relative to different receivers are: $[75.8\ m, 76.7\ m]$ relative to the transmitter-receiver 1 pair, $[56.5\ m, 56.75\ m]$ relative to the transmitter-receiver 2 pair and $[53.13\ m, 54.28\ m]$ relative to the transmitter-receiver 3 pair.

A stationary extended clutter is also present as shown in Fig. 2, its bistatic range extents are given by: $[23.84\ m, 24.66\ m]$ relative to the transmitter-receiver 1 pair, $[28.46\ m, 29.31\ m]$ relative to the transmitter-receiver 2 pair and $[17.71\ m, 18.09\ m]$ relative to the transmitter-receiver 3 pair. The Signal-To-Clutter ratio (SCR) is assumed the same at each receiver and equal

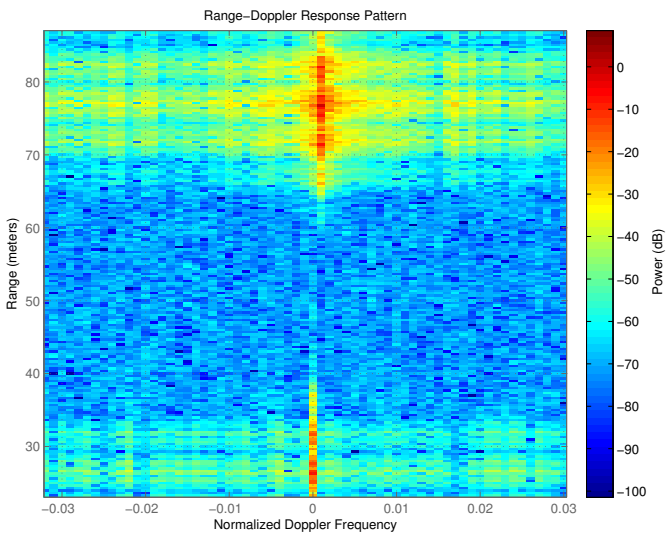

(a) Range-Doppler map at receiver 1

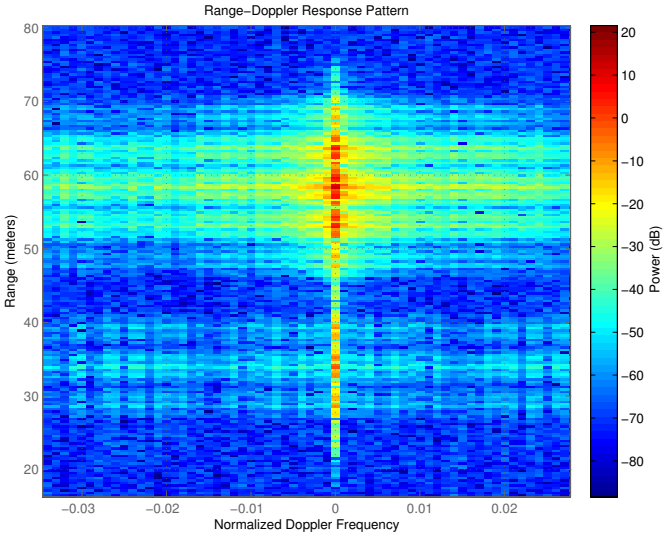

(b) Range-Doppler map at receiver 2

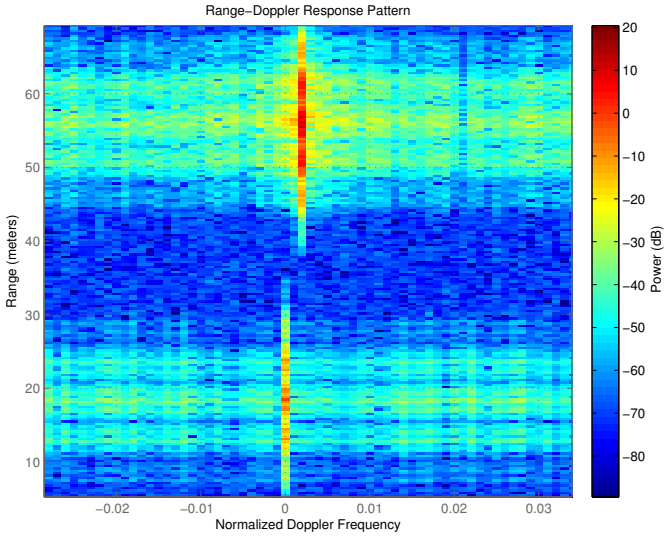

(c) Range-Doppler map at receiver 3

Fig. 2. Bistatic range-Doppler maps.

to 13.97 dB. An Additive White Gaussian Noise (AWGN) is added to the received signals prior to match filtering. The SNR at each receiver is chosen to be 26.98 dB.

As seen from Fig. 2, using Hadamard sequences of sufficient length (N = 512) allows us to have higher integration time, which results in better Doppler resolution. Neverthless, due to the nature of the transmitted waveform (i.e., a train of phase-coded pulses), additional peaks nearby the target responses are generated from range sidelobes. We have noticed that these peaks are at least 20 dB lower than the target responses and they have a low impact on the target detection performance as validated by the detection results in the following section.

B. Probability of Target Detection

Fig. 3 depicts the probability of target detection in the presence of AWGN and clutter interference. The SCNR expressed in (16) is used to evaluate the probability of target detection, since this expression takes into account the extended target impulse

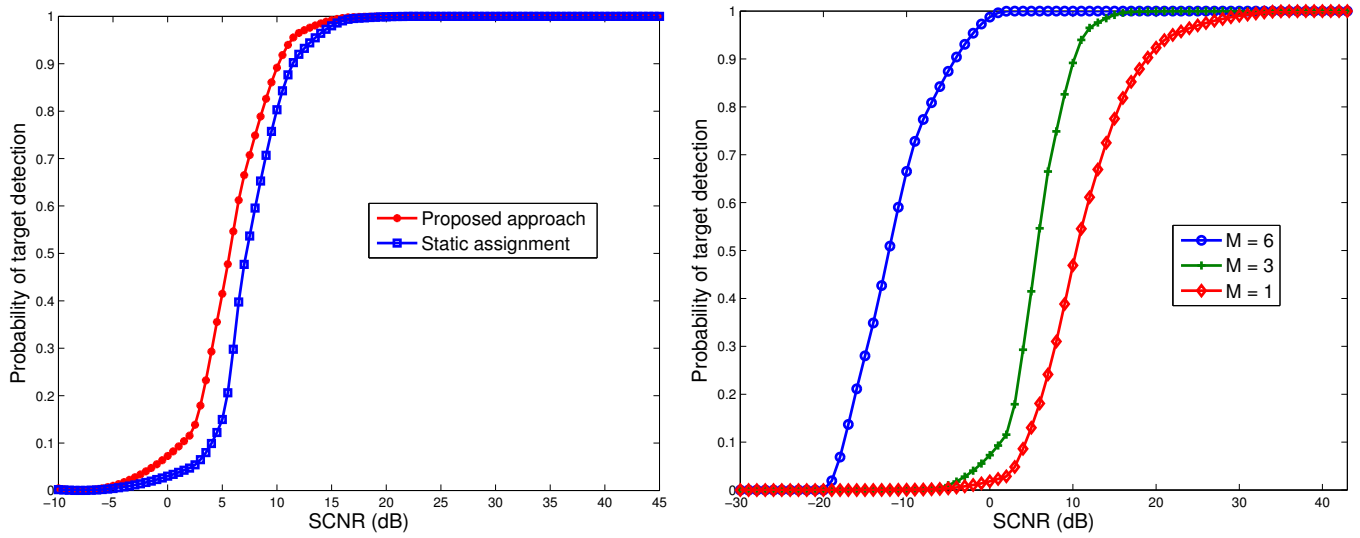

(a) (b)

Fig. 3. (a) Probability of target detection for waveform selection approach and static waveform assignment, (b) Probability of target detection for waveform selection approach with different number of receivers (M = 1, 3 and 6).

responses and scattering characteristics, in addition to clutter and noise covariance.

For each value of SCNR, the threshold γ is computed in order to ensure a fixed probability of false alarm equal to 10^{-5}, then the probability of detection is computed based on (12). In the simulations context, we assume that all the receivers have the same SCNR.

In Fig. 3(a), we compare the values of the probability of detection for the cognitive selection of waveforms that maximize the probability of detection to the values for an arbitrary static waveform. As the proposed approach adapts the choice of waveform to the dynamic scene (i.e., the target RCS fluctuations and the clutter distribution), better detection performances are illustrated compared to the static assignment case where the waveform is unable to match the time-varying target response.

Fig. 3(b) depicts the gain in target detection when multiple spatially separated receivers are used compared to a single receiver case. An improvement in the probability of target detection is illustrated for increased number of receivers as predicted from (12) where we clearly see the spatial diversity contribution of the multistatic topology in detection performances.

C. LS Geolocation Process

Fig. 4 shows the Cumulative Distribution Function (CDF) of the target absolute position error in both cases where static receiver locations are used and GDOP based receiver locations update is applied. The CDF curves are obtained by simulating different values of the target position over an entire area of $150\ m \times 150\ m$ and storing the estimated values by the LS geolocation process. The error is computed as the Euclidean distance between the true and the estimated values. We can notice that better target positioning accuracy is achieved by the receivers placement update mechanism compared to the case of static receivers.

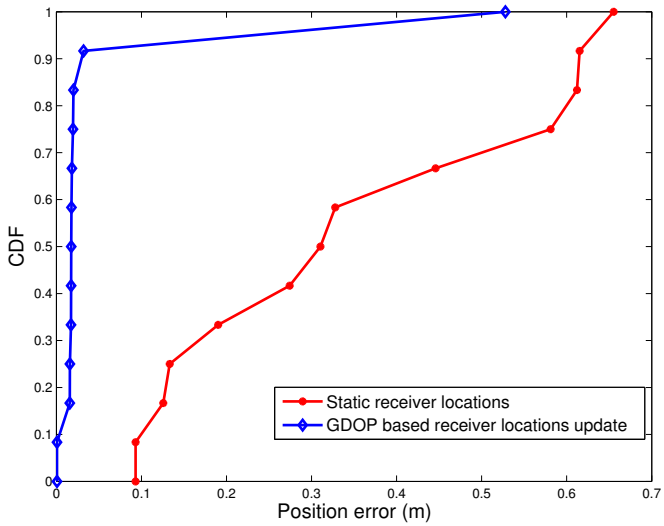

Fig. 4. CDF of the target position estimate error.

D. GDOP based receiver locations Update

Fig. 5 shows the improvement in GDOP values as a function of the number of algorithm iterations considering the GDOP minimization problem of (30). The locations of different receivers are first chosen randomly, then we run the GDOP minimization algorithm according to the current target position estimate. All along the processing duration, the algorithm search iteratively for the optimal receiver locations that minimize the GDOP value within specific error tolerance constraints. As we can see from Fig. 5, the achieved GDOP value is less than $1\ m$ starting from the 17^{th} iteration.

Fig. 6 shows the receiver positions computed by the GDOP optimization process at iterations 1, 5, 10, 15 and 20 (the index "i" refers to iteration count) as depicted in Fig. 5. The transmitter is placed at the origin and the target position is kept the same during the iterative GDOP optimization process. Fig. 6(b) shows the 2-D projection for receiver location updates over iterations onto the x-y plane.

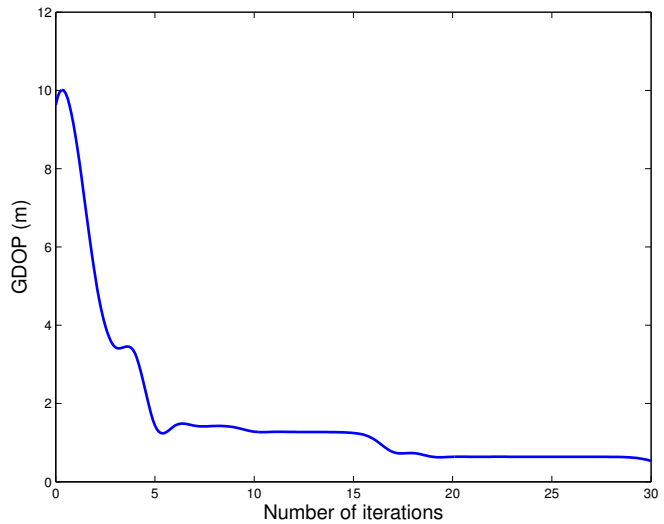

Fig. 5. GDOP iterative minimization process.

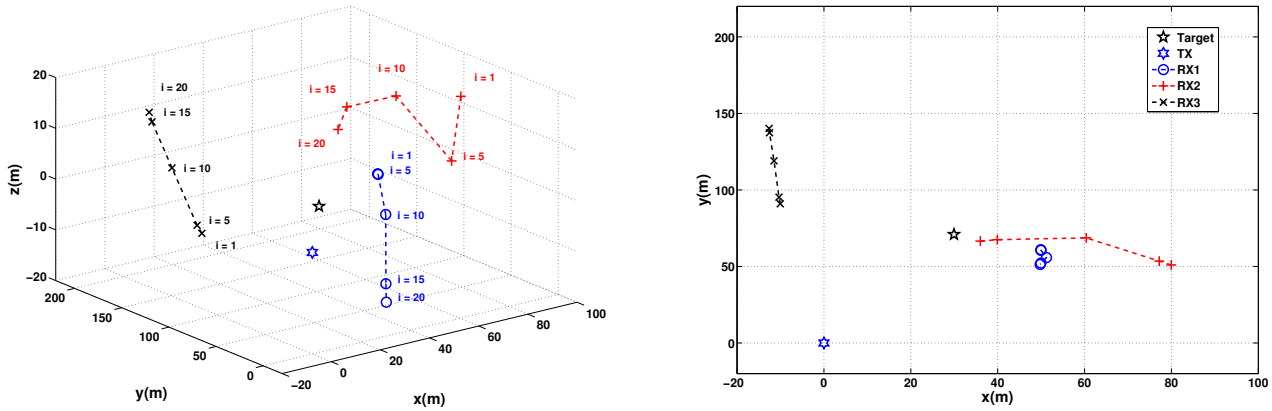

(a) (b)

Fig. 6. (a) 3-D receiver location updates over iterations, (b) 2-D projection for receiver location updates over iterations.

E. Joint Approach Detection Performance

Fig. 7 depicts the Receiver Operating Characteristics (ROC) curves in both cases where only waveform selection based on detection maximization process is carried out, and the proposed approach of waveform selection based on detection maximization in conjunction with adaptive receiver locations selection mechanism is used. We deliberately choose low SCNR values at different receivers in order to study the impact of the adaptive receiver allocation on the overall system detection performances (the used SCNR is equal to -5 dB at each receiver). Low SCNR values cause a drop on the detection performances, but as we can see from Fig. 7, the GDOP based receiver locations update process allows a better target positioning accuracy, which results in detection performance enhancement.

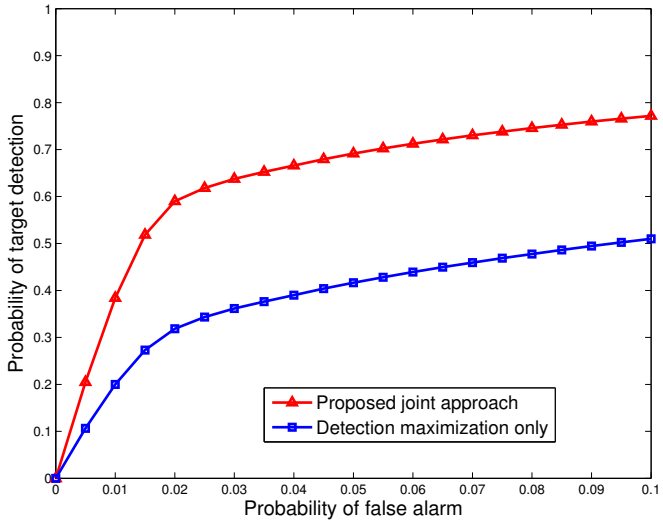

Fig. 7. Low SCNR ROC curves for the proposed approach and the detection maximization process.

F. Multistatic Ambiguity Function

The Ambiguity Function (AF) is a practical tool to verify the suitability of the transmitted waveforms to the system requirements. In fact, the capability of the radar system to resolve two present targets is determined by the half-power width

of the ambiguity function main lobe, while the accuracy of a specific target estimation is dictated by the sharpness of the main lobe [17].

In bistatic configuration, the relationships between delay-Doppler and range velocity pairs are non-linear [22]. If the transmitter is chosen as the reference point, the bistatic AF can be expressed as [22]:

$$\begin{aligned}&\theta(R_{T_h}, R_{T_a}, V_h\cos\phi, V_a\cos\phi, \theta_T, L)\\ =&\left|\int_{-\infty}^{\infty} s(t-\tau_a(R_{T_a},\theta_T,L))s^*(t-\tau_h(R_{T_h},\theta_T,L))\right.\\ &\times\exp[-j(f_h(R_{T_h},V_h\cos\phi,\theta_T,L)\\ &\left.-f_a(R_{T_a},V_a\cos\phi,\theta_T,L))t]dt\right|^2,\end{aligned} \tag{31}$$

where the subscripts a and h are used to denote respectively the actual and the hypothesized values of the parameter associated with the target, f is the bistatic Doppler shift already expressed in (19) and τ is the bistatic delay expressed as [22]:

$$\tau(R_T,\theta_T,L)=\left[R_T+\sqrt{R_T^2+L^2-2R_TL\sin\theta_T}\right]/c, \tag{32}$$

where c is the wave propagation speed.

We can notice from (19), (31) and (32) that the bistatic AF depends on the bistatic geometry in addition to the transmitted waveform. In case of multiple widely-spaced receivers and fluctuating extended target, the signal fluctuations are independent at different receivers and the notion of multistatic AF is defined according to [9], [23] as a weighting combination of bistatic ambiguity functions related to different transmitter-receiver pairs. The weights used to form the multistatic AF are directly related to the SCNR at each receiver [9], [23] and depend on the target scattering characteristics.

We consider a Swerling I extended target composed of seven powerful scattering points. The absolute range extent of the target is about $1\ m$ and the target scattering center is located at $(30\ m, 71\ m, 0\ m)$. We assume three receivers with equal SCNR.

We plot in Fig. 8(a) the multistatic ambiguity function after applying the proposed approach: we jointly select the waveform that maximizes the multistatic probability of detection expression in (12) according to the target impulse responses in addition to the clutter plus noise estimates. Meanwhile the receivers are moved to the optimal locations, which are dictated by the GDOP minimization process. The optimal receiver locations are computed according to the target scattering center estimate. On the other hand, we plot in Fig. 8(b) the multistatic ambiguity function related to a random choice of waveform and receivers placement. It is clearly seen that the proposed cognitive approach offers more target accuracy (i.e., sharpness of the main lobe) than any random assignment of waveform and receiver locations.

VI. Conclusions

We have presented a practical framework for joint cognitive waveform selection and adaptive GDOP based receiver locations update strategy. Relevant information about the real-time extended target impulse responses in addition to the clutter plus noise covariance estimates are processed by the central processor each time backscattered signals are sent from different receivers.

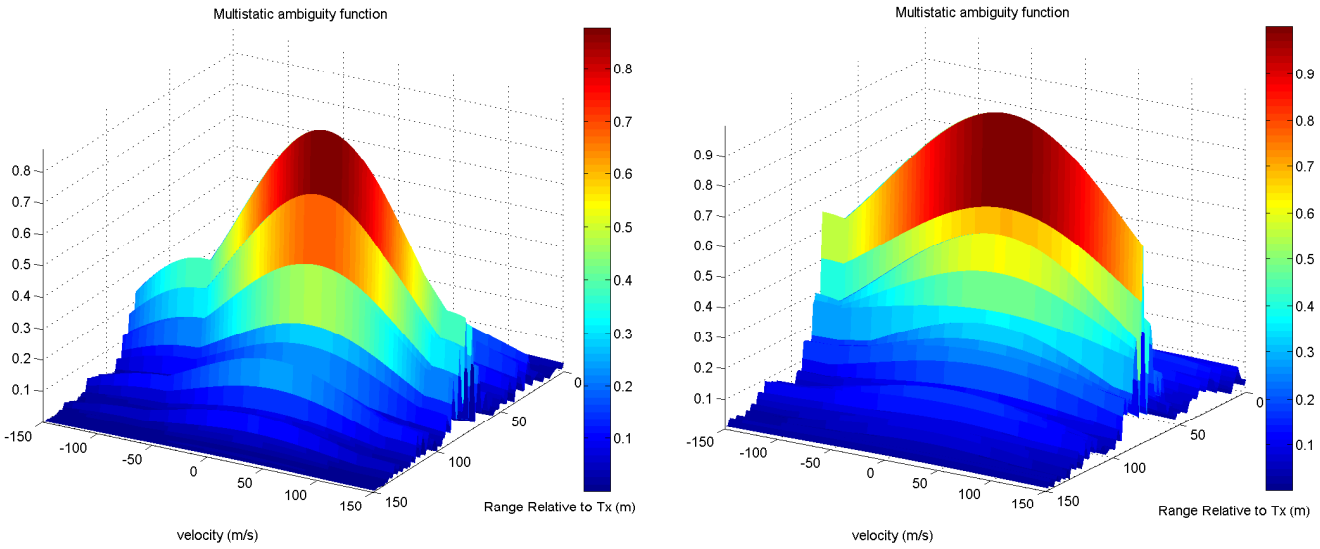

(a) (b)

Fig. 8. (a) Multistatic AF using the proposed approach, (b) Multistatic AF with a random choice of waveform and receivers placement.

Maximization of the target probability of detection is carried out in the central processor to select the optimal waveform, meanwhile the target position estimate obtained from the LS geolocation algorithm is forwarded to a GDOP minimization process, which compute the optimal locations of the receivers that maximize the target positioning accuracy. The destined commands for the transmitter and the receivers are then sent simultaneously and the multistatic radar is able to quickly adapt to the dynamically changing environment. Optimal system performance is conditioned by synchronization between waveform selection and receivers placement strategy, which should be controlled at the processor level. The proposed approach leverage the benefits of multistatic topology, especially the spatial diversity and the wider coverage, to enhance the extended target probability of detection in the presence of clutter and noise. On the other hand, the receivers are able to move within specific areas to maximize the target positioning accuracy. From a practical point of view, the proposed approach is suitable for a moving multistatic platforms as is the case of Unmanned Aerial Vehicle (UAV) based multistatic topology, or moving radar platforms during tactical military missions.

ACKNOWLEDGEMENT

This work was supported by the Natural Sciences and Engineering Research Council of Canada (NSERC).

REFERENCES

[1] Haykin, S.: 'Cognitive radar: a way of the future', IEEE Signal Process. Mag., 2006, 23, (1), pp. 1−7

[2] Pillai, S.U., Oh, H.S., Youla, D.C., Guerci, J.R.: 'Optimal transmit-receiver design in the presence of signal-dependent interference and channel noise, IEEE Trans. Inf. Theory., 2000, 46, (2), pp. 577−584

[3] Garren, D.A., Osborn, M.K., Odom, A.C., Goldstein, J.S., Pillai, S.U., Guerci, J.R.: 'Enhanced target detection and identification via optimised radar transmission pulse shape', IEE Proc., Radar Sonar Navig., 2001, 148, (3), pp. 130−138

[4] Estephan, H., Amin, M.G., Yemelyanov, K.M.: 'Optimal waveform design for improved indoor target detection in sensing through-the-wall applications', IEEE Trans. Geosci. Remote Sens., 2010, 48, (7), pp. 2930−2941

[5] Kay, S.: 'Waveform design for multistatic radar detection', IEEE Trans. Aerosp. Electron. Syst., 2009, 45, (3), pp. 1153−1166

[6] Jun, L., Hongbin, L., Himed, B.: 'Two target detection algorithms for passive multistatic radar', IEEE Trans. Signal Process., 2014, 62, (22), pp. 5930−5939

[7] Bruyere, D., Goodman, N.: 'Adaptive detection and diversity order in multistatic radar', IEEE Trans. Aerosp. Electron. Syst., 2008, 44, (4), pp.1615−1623

[8] Stinco, P., Greco, M.S., Gini, F., and Manna, M.L.: 'Non-cooperative target recognition in multistatic radar systems', IET Radar, Sonar Navig., 2014, 8, (4), pp. 396−405

[9] Derham, T., Doughty, S., Baker, C., K. Woodbridge, K.: 'Ambiguity functions for spatially coherent and incoherent multistatic radar', IEEE Trans. Aerosp. Electron. Syst., 2010, 46, (1), pp. 230−245

[10] Yarlagadda, R., Ali, I., Al-Dhahir, N., Hershey, J.: 'GPS GDOP metric', IET Radar, Sonar Navig., 2000, 147, (5), pp. 259−264

[11] Sharp, I., Kegen, Y., Guo, Y.J.: 'GDOP analysis for positioning system design', IEEE Trans. Veh. Technol., 2009, 58, (7), pp. 3371−3382

[12] Torrieri, D.J.: 'Statistical theory of passive location systems', IEEE Trans. Aerosp. Electron. Syst., 1984, AES-20, (2), pp. 183−198

[13] Sharp, I., Yu, K., Hedley, M.: 'On the GDOP and accuracy for indoor positioning', IEEE Trans. Aerosp. Electron. Syst., 2012, 48, (3), pp. 2032−2051

[14] Anastasio, V., Colone, F., Di Lallo, A., Farina, A., Gumiero, F., Lombardo, P.: 'Optimization of multistatic passive radar geometry based on crlb with uncertain observations', in Proc. 2010 European Radar Conf. (EuRAD), Paris, France, 2010, pp. 340−343

[15] Gumiero, F., Santarelli, S., Bongioanni, C., Colone, F., Lombardo, P.: 'Using real data for the implementation of multistatic passive radar geometry optimization procedure', in Proc. 2011 European Radar Conf. (EuRAD), Manchester, England, October 2011, pp. 93−96

[16] Nguyen, N.H., Dogancay, K., Davis, L.M.: 'Joint transmitter waveform and receiver path optimization for target tracking by multistatic radar system', in IEEE Workshop on Statistical Signal Processing (SSP), Gold Coast, VIC, 2014, pp. 444−447

[17] Skolnik, M.: ' Radar Handbook'(McGraw Hill, 3rd edn. 2008)

[18] Sorensen, D.C.: 'Newtons method with a model trust region modification', SIAM Journal on Numerical Analysis, 1982, 19, (2), pp. 409−426

[19] Chen, C.H., Feng, K.T., Chen, C.L., Tseng, P.H.: 'Wireless location estimation with the assistance of virtual base stations', IEEE Trans. Veh. Technol., 2009, 58, (1), pp. 93−106

[20] Waltz, R.A., Morales, J.L., Nocedal, J., Orban, D.: 'An interior algorithm for nonlinear optimization that combines line search and trust region steps', Mathematical Programming Journal, 2006, 107, (3), pp. 391−408

[21] Bell, M.: 'Information theory and radar waveform design', IEEE Trans. Inf. Theory, 1993, 39, (5), pp. 1578−1597

[22] Tsao, T., Slamani, M., Varshney, P., Weiner, D., Schwarzlander, H., Borek, S.: 'Ambiguity function for a bistatic radar', IEEE Trans. Aerosp. Electron. Syst., 1997, 33, (3), pp. 1041−1051

[23] Bradaric, I., Capraro, G.T., Weiner, D.D., Wicks, M.C.: 'Multistatic radar systems signal processing', in IEEE Conference on Radar, 2006